Journal of Autonomous Intelligence (2023) Volume 6 Issue 3
doi: 10.32629/jai.v6i3.698

ORIGINAL RESEARCH ARTICLE

AI-based COVID-19 disease detection in medical images: Advancements and implications in healthcare

Navneet Kaur

Chitkara University School of Engineering & Technology, Chitkara University, Himachal Pradesh 174103, India; navneet.kaur_cse@chitkarauniversity.edu.in

ABSTRACT

Medical image analysis and categorization have seen success using artificial intelligence (AI) approaches and convolutional neural networks (CNNs). The diagnosis of COVID-19 based on the classification of chest X-ray images has been proposed in this research using a deep CNN architecture. Since there was no dataset of chest X-ray pictures that was sufficiently large and of high quality, it was difficult to execute a reliable and accurate CNN classification. The dataset is preprocessed utilizing several stages and procedures to build an acceptable training set for suggested CNN model to reach its optimal performance. This was carried out to address these complications, including the accessibility of a tiny, unbalanced dataset with poor photo quality. The datasets employed in this study included preprocessing processes such as medical image analysis, dataset balance, and data augmentation (DA). The simulation outcomes showed an accuracy of 99.80%, highlighting the strength of presented scheme in the specified application field. The comparative study used in the paper is conducted with a few ML algorithms that demonstrates the outperformance of the suggested scheme in comparison with other schemes in terms of various performance parameters. Additionally, two diagnostic tools, i.e., receiver operating characteristic (ROC) curve and precision-recall curve, that aid in the understanding of probabilistic forecast for binary (two-class) classification predictive modelling issues are also displayed in this article.

Keywords: medical images; CNN model; COVID-19; accuracy

ARTICLE INFO

Received: 12 June 2023
Accepted: 26 July 2023
Available online: 27 September 2023

1. Introduction

In late 2019, the severe acute respiratory syndrome coronavirus 2 (SARS-CoV-2) virus had been identified. A virus with its roots in China was the cause of the COVID-19[1]. By March 2020, the virus was categorized as a pandemic by WHO. The epidemic reportedly tormented millions of people around the world, according to reports released and updated by state governments and international healthcare organizations[2–3]. The most severe sickness brought on by COVID-19 is lung-related, such as pneumonia. A few of the disease's symptoms are dyspnea, a high fever, a runny nose, and a cough. The most frequent method for diagnosing these patients is through looking for anomalies on chest X-ray images[1–4]. The term "X-ray" refers to electromagnetic penetrating radiation. To produce photographs of the inside intricacies of the body part, these radiations are delivered via targeted human body parts. X-ray photographing produces a monochromatic representation of internal bodily structures, with areas of different densities appearing as shades of black and white. This technique is considered one of the earliest and most commonly utilized strategies for medical diagnosis. A radiographic photograph of the thoracic cavity is obtained through a chest X-ray, revealing the bony structures of the spine and chest, as

well as the presence of soft tissue components like the lungs, and airways. The diagnosis of lung and chest-related conditions, such as pneumonia, is made using this imaging[5]. X-ray imaging offers numerous advantages over traditional strategies as a substitute diagnostic strategy for COVID-19 testing. These reimbursements embrace the abundance of X-ray facilities, the non-invasiveness, shot time commitment, and low cost. Consequently, in healthcare crisis, X-ray photographing can be thought of as a desirable choice for speedy diagnosis strategy for an epidemic like COVID-19.

Over past ten years, research has shifted exponentially towards deep learning (DL) and ANNs. On many crucial criteria, deep ANNs have outperformed other traditional models. Thus, ANNs have typically been shown to be the cutting-edge strategy across a broad spectrum of application sectors, including voice recognition, biological research, image processing, and other commercial and educational fields. The development of ANNs has enormous promise for medical applications, particularly in the analysis and interpretation of medical picture data. As has been observed recently, there is a global healthcare crisis that affects both the required quantity of healthcare personnel and the testing equipment. In light of the current pandemic situation, analysis and classification of chest X-ray pictures and the detection of COVID-19 patients are proximate. In this study, CNN has been used to create an automatic diagnostic system that determines if a person has COVID-19 or not based on the findings of a chest X-ray analysis.

Healthcare uses for DL have risen substantially, especially in image-based diagnosis. Other conventional image analysis algorithms and methods were surpassed by ANNs[6,7], and DL frameworks performed satisfactorily in computer vision problems pertaining to healthcare image analysis. CNNs are regarded as the de facto standard in this field due to the extremely encouraging results they have produced in healthcare image analysis and classification[8,9]. CNN is employed for a number of classification responsibilities related to healthcare verdicts, including interstitial lung disease, breast cancer recognition, wireless endoscopy images, interstitial lung disease, lung disease, and malarial pathogen identification[10–15]. Numerous researchers have been working on experiments and research projects relevant to the diagnosis, treatment, and management of COVID-19 ever since it first surfaced in December 2019.

The importance of using AI techniques for picture scrutiny for the recognition and supervision of COVID-19 cases has been described by Dong et al.[16]. By analyzing pulmonary CT data with DL models, COVID-19 can be detected with accuracy[16]. Wang and Wong[17] have created a deep CNN-based freely available COVID-19 diagnosing platform. The recognition of COVID-19 patients employing X-ray pictures is stated in this study utilizing a customized CNN outline. Another significant work by Apostolopoulos and Mpesiana[18] discussed the X-ray dataset, including pictures from people with common pneumonia, COVID-19 patients, and healthy individuals. The study employs cutting-edge CNN frameworks for the automatic recognition of COVID-19 patients with 97.82% accuracy. Another recent and pertinent work examined the validity and adaptability of deep CNNs of the Decompose-, Transfer-, and Compose types for the identification of COVID-19 utilizing categorization of chest X-ray images Abbas et al.[19]. The accuracy, sensitivity, and specificity of the authors' reporting of the study's findings were 95.12%, 97.91%, and 91.87% respectively. Narin et al.[20] has employed a three-fold binary classification approach, encompassing four distinct classes: COVID-19, normal (healthy), viral pneumonia, and bacterial pneumonia. This classification was performed through the utilization of five-fold cross-validation. Islam et al.[21] have utilized Long Short-Term Memory (LSTM) to analyze extracted features that distinguish COVID-19 cases from non-COVID-19 cases. Despite achieving an accuracy rate, the developed system is limited by its relatively small sample size. Shorfuzzaman et al.[22] proposed a novel fusion framework, which utilizes CNN and deep learning techniques. The framework incorporates the concept of transfer learning, where parameters (weights) from multiple models are integrated into a unified model. This unified model is then employed to extract features from images, which are subsequently inputted into a customized classifier for prediction.

This study's preliminary research has produced encouraging consequences in terms of several performance metrics for timely and affordably diagnosing the condition. In order to increase the COVID-19 X-ray picture classification accuracy, this study applied CNN with various layers. The CNN structure in neural networks is specifically made to handle tasks involving 2D image processing, while it might be applied to 1D and 3D data. First, the dataset[23] has been downloaded to train the CNN model. As dataset poised for training CNN is quite tiny and unbalanced, it is prolonged via DA procedures to improve its size and to make the model training feature rich. This resolved the problem of having very-limited sized X-ray picture dataset. In order to produce more data, images have been rotated and flipped at various angles. The CNN model's performance is evaluated using a variety of performance metrics. These measures include F_1 score, ROC, F_2 score, true positive rate (TPR), accuracy, true negative rate (TNR), false positive rate (FPR), precision (P), and false negative rate (FNR). To demonstrate the significance of the suggested CNN model over other ML models, several other ML models are employed for the comparative examination. Some of the research's major insights are as follows:

- The performance of the suggested CNN model is extremely remarkable as compared to other ML strategies in terms of various performance parameters like precision, TPR, TNR, FPR, FNR, F_1 score, F_2 score.
- The proposed binary classification model has been diagnosed using ROC curves and precision-recall curves.
- By integrating X-rays and CNN-based evaluation, the medical sector can manage widespread surveillance eventualities in pandemics like COVID-19.
- With the usage of DA procedures, it is conceivable to ominously boost the CNN model's performance by addition of more data to a dataset that is currently of a small size. Image classification gains benefits from DA.

The remainder of the paper is broken up into several sections. Section 2 provides a clear elucidation of the materials and procedures employed. Section 3 of the research presents its results, the discussion is covered in section 4, and its conclusion is then presented in section 5.

2. Materials and methods

The overview of this research is shown in **Figure 1** and starts with the gathering of a principal dataset with two picture classes: one comprised chest X-rays obtained from patients diagnosed with COVID-19, whereas the other consisted of images obtained from individuals deemed healthy. The concerned medical experts examined the dataset during the study's following phase and eliminated some of the X-ray pictures that lacked clarity regarding quality and analytical norms.

The data collection obtained exhibits an outstanding level of cleanliness owing to the fact every X-ray picture is of superior quality and exhibits clarity with respect to crucial diagnostic features based on the expertise of the professionals involved. In the third stage, the dataset is expanded via conventional augmentation procedures. In the following stage, the model was trained using the resultant dataset. Following training, the model's capability to identify diseases has been assessed. Both the independent validation dataset and the test dataset taken from the main dataset have been utilized to test the suggested CNN model. The detailed structure of presented research is shown in **Figure 2**.

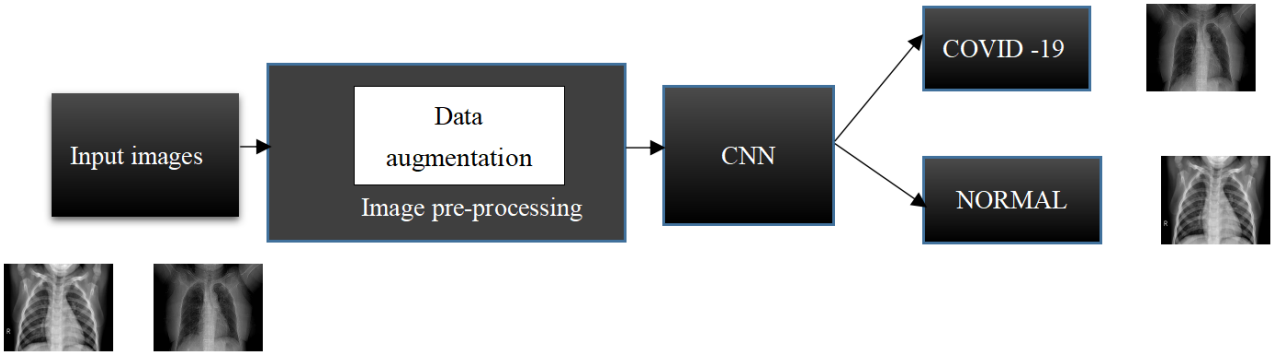

Figure 1. Overview of the proposed scheme.

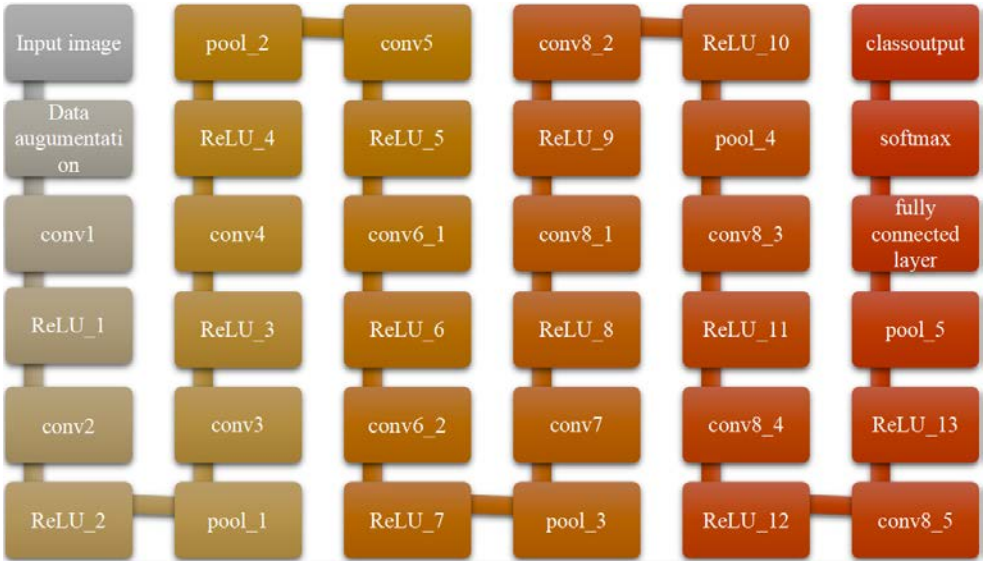

Figure 2. The detailed architecture of the proposed scheme.

A dataset of X-ray photographs has served as a basis for the present research. Of those photos, some are of proven COVID-19 patients, while the remaining are of healthy individuals or those suffering from other illnesses, such as pneumonia. The dataset is imbalanced and requires preprocessing to produce satisfactory findings. As an initial effort, CNN is trained on provided original dataset with an accuracy of about 54%, which is unsuitable for the application domain at hand. Some pictures are employed to equalize the presented dataset to enhance the efficacy of the suggested schemes. The accuracy of the provided CNN models increased to 69% after the dataset was balanced and the models were retrained on the resulting dataset. However, the models' accuracy and other results did not support their claim to be a reliable approach for COVID-19 detection[23].

The X-ray scans were thoroughly examined by medical professionals. A collection of X-ray photos has been designated as the ideal aspirant to train the models out of some X-ray pictures of individuals having COVID-19[24]. The ultimate dataset comprised of validated instances of COVID-19 and conventional X-ray photographs. The proposed CNN model is once more trained using the resulting dataset, and this time the model's performance improved. In the aforementioned circumstance, the accuracy specifically rose to 72%. However, the accuracy and other performance indicators did not much improve because the dataset lacked enough images for efficient training.

A method known as DA allows users to greatly enhance total data scenarios in a dataset employed for model training[24]. The technique smears standard image processing procedures to image collections, alike flipping, cropping, or rotating for augmentation.

The dataset is further expanded by these altered pictures that are produced from the original image set,

enhancing the dataset size for training deep neural networks (DNN)[25]. The DA system has been applied to address the issue of obtainability of a tiny dataset that is impacting the efficacy of the suggested scheme. Further, it is made larger using this strategy, which also offers the learning system novel learning attributes.

The visual system of the human brain served as inspiration for CNN. Making computers capable of seeing the world like people do is the goal underlying CNNs. CNN can be utilized in this fashion in the fields of visual analysis, categorization, and NLP[26]. CNNs are DNN featuring nonlinear activation, convolutional, and max pooling layers. The "convolution" maneuver, which gives CNN its name, is carried out by the convolutional layer, which is regarded as one of its key layers. The convolutional layer's inputs are subjected to its kernels. A feature map is created by convolving all of the convolutional layer outputs. The utilization of Rectified Linear Unit (ReLU) as a function of activation in conjunction with a convolutional layer is employed in this research to enhance the irregularity of the input photo, as photographs are intrinsically nonlinear. CNN with ReLU is therefore simpler and faster in the current situation.

The pooling layer, which is alternatively referred to as the subsampling layer, constitutes a pivotal component of the CNN. It functions self-reliantly on each feature map that is excavated via convolution layer. It reduces the feature map's size and yields the critical structures to reduce overfitting and the amount of excavated features. In the CNN model, pooling might be the maximum, average, and sum. Because max pooling makes it easier to spot the sharp features than other methods, it was chosen for this investigation. Additionally, as this study included training a DNN, the batch normalization layer is utilized[26]. The strategy alters both scaling and activation in order to normalize the input layer and expedite learning among hidden components. In order to combat overfitting, a dropout layer is employed, that eliminates the neurons selected at random during training[27,28].

The proposed CNN model has 34 layers, 13 of which are convolutional (Conv2D), 13 ReLU layers, 5 layers of maximum pooling, 1 fully connected layer, 1 layer of softmax, and 1 layer that acts as the output layer. 64 high-pass filters of size 3 × 3 × 3 are used to initialize the weights in the first convolutional layer. As a result, there are 3 × 3 × 3 × 64 = 1728 weights in total for the first convolutional layer. Consequently, the weight of apiece layer can be categorized depending on size, quantity, and description of the preceding layer. As, layer 7 has 3 × 3 × 64 × 128 weights, which denotes that the filter size is 3, the number of filters used in the current layer is 1, and the number of filters used in the layer before it was 64. The total weight in this case can be computed using the formula 3 × 3 × 64 × 128 = 73,728 weights.

The CNN was employed in the early trials in a variety of configurations with regard to the number of convolutional layers employed in the model. The CNN is first put to the test with a solitary convolutional layer, and consequences are inspected. The CNN is assembled in 2 layers, consequences are gauged, and so forth. The method is continued until the consequences of the strategy produced are precise and efficient. The final strategy, which contained 13 convolution layers, is very practicable according to its results, which are reported in the results section.

3. Results

A thorough evaluation of the outcomes produced by the suggested method is provided in the section that follows. The obtained results are also contrasted with the earlier findings reported in the literature section. Additionally, the suggested technique's resistance to various geometrical attacks is assessed and contrasted with other methods. MATLAB R2020a (9.8.0.1417392) is used to run the suggested system. Microsoft Windows 8.1 running on a 64-bit operating system with 8.00 GB of memory is used to run the simulation.

Several performance indicators are used to rate the suggested algorithm. Accuracy is the proportion of the total images' T_P and T_N sum to the total pictures. Precision is the chance that the detected image is a forgery.

TPR, sensitivity, or recall (R) are terms used to describe the capacity to identify a forged image as a fake one. TNR or specificity are terms used to define the capacity to recognize an authentic image as authentic. The average of recall and precision is the F_1 score. The recall and precision of the F_2 score are average. The missing detection rate for the forged region is represented by the FNR. For improving performance, lower values for this parameter are much preferable. FPR is the percentage of false positives that are not identified[29–31].

$$Accuracy = \frac{T_P + T_N}{F_P + T_P + F_N + T_N} \tag{1}$$

$$P = \frac{T_P}{F_P + T_P} \tag{2}$$

$$TPR = R = \frac{T_P}{F_N + T_P} \tag{3}$$

$$TNR = \frac{T_N}{T_N + F_P} \tag{4}$$

$$F_1 score = 2\frac{P \times R}{P + R} \tag{5}$$

$$F_2 score = 5\frac{P \times R}{4 \times P + R} \tag{6}$$

$$FNR = \frac{F_N}{F_N + T_P} \tag{7}$$

$$FPR = \frac{F_P}{F_P + T_N} \tag{8}$$

where T_P stands for the total number of photos that were accurately identified as fake, F_P for the total number of fake photos that were incorrectly recognized, F_N for the number of fake pictures that were missed, and T_N for the total number of real images that were accurately identified as real.

The final dataset has 1400 X-ray pictures in total after preprocessing. The dataset was divided into two subsets for the purposes of training and testing the suggested CNN. The testing dataset had 500 X-ray photos, of which 250 are from apiece class (Normal and COVID-19), totaling 500 X-ray photos. The training set comprises 380 COVID-19 X-ray photos and 380 normal X-ray photos. 140 X-ray pictures from the training subset were then given to the model along with a 10% validation size. Thus, each epoch uses 720 X-ray photos to train the model and 500 X-ray photos to authenticate it out of a total of 140 X-ray pictures.

To determine the total number of epochs that offer the best performance, several tests have been run utilizing various epochs. Prior to model training, the dataset is randomly organized into test, train, and validation sets. A validation set is used to evaluate the model after each training cycle. The cessation of the training process occurs when the model's performance on the validation set exhibits a decline, such as a rise in loss or a drop in accuracy, or when it reaches a plateau. Early halting is a technique used to address the problem of overfitting the data. The learning rate is a hyperparameter that governs the extent to which the model is modified in reaction to anticipated error during each iteration of CNN training when the model weights are adjusted. It normally falls between 0.0 and 1.0, and it has a small positive number. The size of the mini-batch in the suggested method is 32, and the learning rate is 0.0001.

The dataset's results for various epochs are shown in **Table 1**. With 90 epochs, the validation set's accuracy increased from 76% to 99.52% while the training set's accuracy increased from 75% to 99.80%. Additionally, both the training loss and the validation loss continue to go down. As the validation accuracy remains persistent after the 90th epoch, as depicted in **Table 1**, the finest performance is attained with 90 epochs. As a result, training procedure ends with a 99.80% accuracy after the 90th epoch.

Table 1. Training consequences obtained by the presented technique.

Epoch	Training accuracy	Training loss	Validation accuracy	Validation loss	Base learning rate
10	75.13%	0.4711	76.00%	0.5550	0.0001
20	90.13%	0.2606	94.33%	0.2551	0.0001
40	92.75%	0.1569	98.50%	0.1209	0.0001
60	93.68%	0.1243	98.67%	0.1083	0.0001
70	95.97%	0.1138	98.83%	0.0949	0.0001
80	97.88%	0.0687	99.52%	0.0504	0.0001
90	99.80%	0.0537	99.52%	0.0512	0.0001

Accuracy and loss plots are used to extensively analyze the performance of the proposed scheme for both training and validation. Our model is probably overfitting if it performs significantly better on the training set than the validation set. These graphs, which represent the model's training quality, are shown in **Figure 3**. Given that the validation set outperforms the training set, the closely related training and validation curves suggest that it is neither overfitting nor underfitting. This shows that with each new step, the model's capacity to generalize to previously unknown data increases. The dataset's training epochs are used to generate the graphs. For evaluating the model's learning and generalization capabilities concurrently in both validation and training sets, accuracy and loss are acquired. It is prominent that accuracy curves first parade an ascending trend until achieving a persistent value at a fact of supreme performance. Similar to this, the training and validation losses in loss plots continue to decline until they reach their minimal value. For the used dataset, 90 epochs yield the best result. The equilibrium between recall and precision at different thresholds is depicted by the precision-recall curve. Plotting the ratio of FPR (on the *x* axis) v/s TPR (on the *y* axis) yields the ROC curve. **Figure 4** illustrates the precision-recall curve and ROC curve for the proposed scheme.

(a)

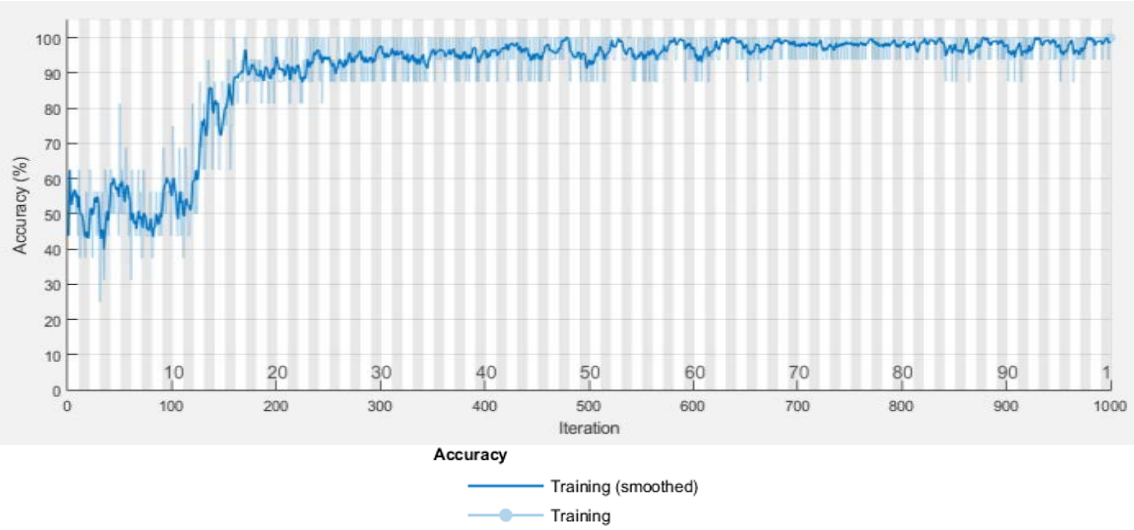

(b)

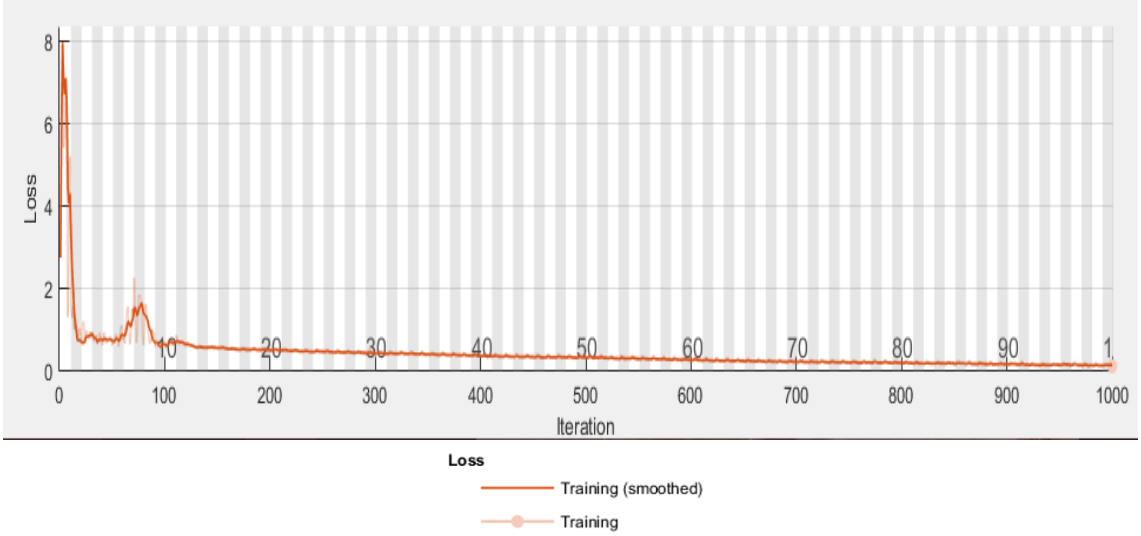

Figure 3. Graph between **(a)** training accuracy and; **(b)** loss of proposed scheme.

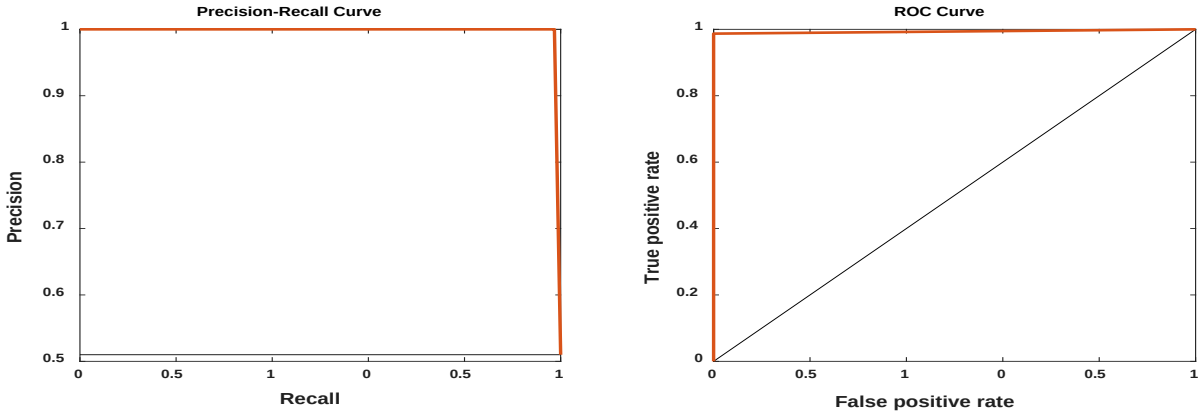

Figure 4. Precision-recall curve and ROC curve of proposed scheme.

The employment of a $P \times P$ matrix, where P represents the total number of target classes, is a common practice for assessing the efficacy of a model, and is commonly referred to as a confusion matrix. The matrix equates the forecast values of the ML model to the real goal values. This paints a flawless depiction of the classification model's accuracy and the types of errors it is generating. Therefore, as shown in **Figure 5**, the effectiveness of the projected methodology is confirmed by confusion matrix. Experts reviewed an image that had been incorrectly categorized. It was observed that the X-ray photograph of an individual in the initial phases of COVID-19 exhibited notable characteristics. The photo lacks the pronounced patterns that would have allowed it to be distinguished from the standard X-ray photo class. The X-ray photograph of a COVID-19 patient that was erroneously classified by the model is depicted in **Figure 6**.

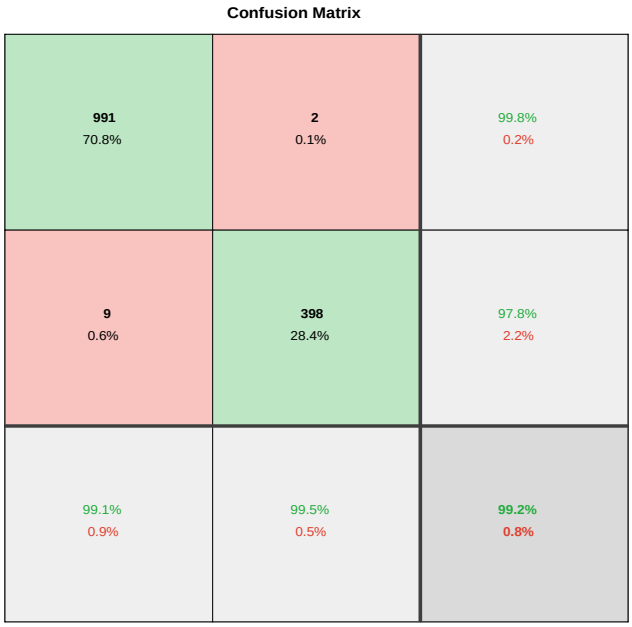

Figure 5. Confusion matrix for the presented study.

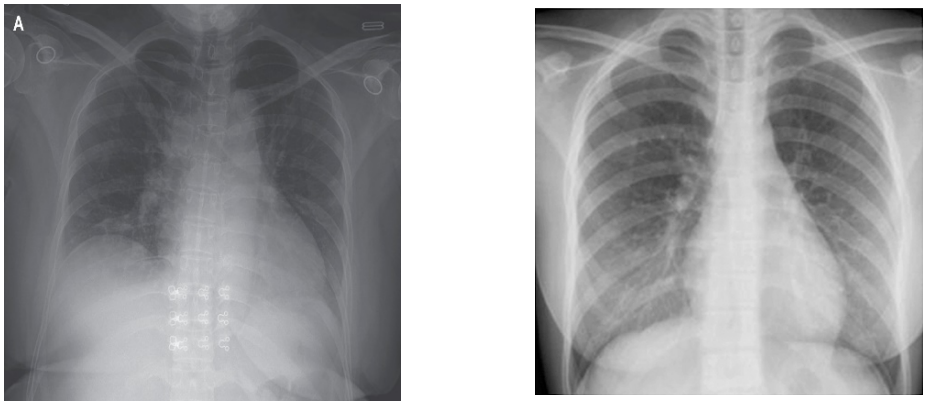

(a) **(b)**

Figure 6. (a) the misclassified X-ray picture; **(b)** correctly classified image.

Several important ML models, including Random Forest (RF), Support Vector classifier (SVC), Logistic Regression (LR), and K-Nearest Neighbour (KNN), have also been the subject of experiments in this work in order to compare CNN with these models[28,32]. Two hyperparameters have been employed with RF. The number of decision trees generated by RF is determined by the n_estimators. The next parameter, denoted as *C*, represents the upper bound on the optimization of SVC algorithm, which serves to mitigate the risk of erroneous of particular training scenarios. SVC is the best for two-class classification. On the contrary, a significantly reduced value of parameter *C* would enhance the optimizer's ability to seek a hyperplane with a wide margin, even if such a hyperplane results in misclassification of some data points. Because LR is preferable when there is a short dataset, it has been utilized using the "liblinear" solver, and the other parameter is *C* as employed in SVC. KNN was applied with all of the default settings. Thus, original dataset from this work was used to train the CNN and ML models. The training subset of the initial dataset is then used to test CNN and ML models[32,33]. As shown in **Table 2**, CNN outperformed these ML models, i.e., SVC, LR, RF, KNN in terms of various performance metrics. Strong proof of the model's potential use in the COVID-19 judgment utilizing X-ray picture cataloging is presented by this comparison study as well as by equating the complete performance consequences obtained by the suggested scheme.

Table 2. Comparison of proposed model with different ML models.

Techniques	Accuracy	Precision	TPR	TNR	F_1	F_2	FNR	FPR
SVC	0.950	0.980	0.895	0.971	0.950	0.958	0.092	0.550
RF	0.961	0.956	0.903	0.940	0.920	0.928	0.060	0.007
KNN	0.923	0.918	0.973	0.982	0.942	0.949	0.020	1.800
LR	0.940	0.925	0.937	0.990	0.930	0.939	0.087	0.009
CNN	0.993	0.987	1.000	0.986	0.993	0.997	0.013	0.000

The bar graph in **Figure 7** compares the performance metrics provided by several machine learning models and CNN. Comparing the proposed CNN model to existing ML algorithms like SVC, LR, RF, and KNN, the figure shows that it performs at high levels for a number of performance measures like accuracy, TPR, TNR, F_1 score, FPR, FPR, and F_2 score. A strong proof of the model's potential usefulness in the COVID-19 diagnosis utilizing X-ray image classification is provided by this comparative study as well as by comparing the overall performance results obtained by the proposed CNN model.

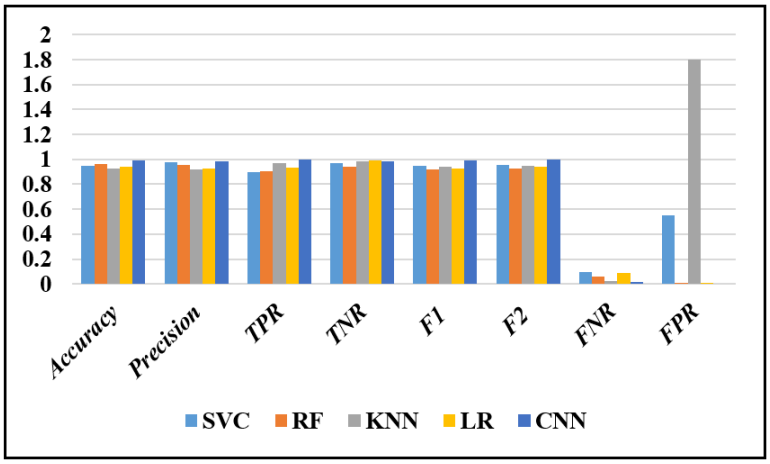

Figure 7. Comparison of various ML algorithms and proposed CNN model.

4. Discussion

This study exhibits the COVID-19's effective judgment using CNN, which was trained on a dataset of chest X-ray images. With datasets, model training is carried out incrementally to get the highest efficacy. The distribution of classes was imbalanced, and the size of the core dataset is severely limited. These two issues with the core dataset severely hindered the performance of the models. To solve these issues, the dataset was preprocessed using a range of techniques, including dataset balancing, physical examination of X-ray images by medical specialists, and DA techniques. To balance the images for training and to evaluate its metrics, numerous chest X-rays are collected from various bases. After training and testing on the completely processed dataset, the effectiveness of the CNN model has been provided.

According to the results from both testing scenarios, the suggested system has shown tremendously promising results. By generating extra data from the current lowest-size dataset, the DA approach aids in enhancing the performance of the anticipated scheme. The CNN algorithm's last iteration consisted of thirteen convolutional layers. Comparisons with a few ML models are made in order to further evaluate the applicability of the proposed strategy. When each model is judged using a different validation dataset, the results show that recommended CNN outperformed other models. Because DA techniques have such a significant impact on model performances, the authors are actively involved in implementing numerous applications of cutting-edge DA algorithms and methodology.

5. Conclusion

Social seclusion and early discovery are the only available preventive measures for the COVID-19 pandemic, a distinct pandemic caused by the coronavirus. The categorization and interpretation of medical imaging data using AI techniques, notably CNNs, has shown remarkable results. The chest X-ray images in this investigation will be classified using a comprehensive CNN architecture in order to find COVID-19. DA techniques are most successful at significantly enhancing the performance of the CNN model by adding additional data to a limited dataset and granting the model the ability to be invariant. The experimental results showed up to 99.80% overall accuracy, demonstrating the strength of the proposed technique in the targeted application domain. ROC curves and Precision-Recall curves are also plotted to identify binary classification models. To further demonstrate that the suggested methodology outperforms other approaches, a comparison with a variety of ML techniques is made, including RF, SVC, LR, and KNN. The findings reveal that the recommended CNN outperformed all other models, particularly when each model was assessed using a different validation dataset.

The authors are actively working on the application of various cutting-edge data augmentation algorithms and methodologies due to the major impact of data augmentation techniques on model performances. The findings of the study on the applicability of these contemporary data augmentation approaches in various application domains will be presented in the future.

Conflict of interest

The author declares no conflict of interest.

Abbreviation

AI	Artificial Intelligence;
CNNs	Convolutional Neural Networks;
COVID-19	Corona Virus Disease 2019;
DA	Data Augmentation;
DN	Deep Learning;
DNN	Deep Neural Networks;
FNR	False Negative Rate;
FPR	False Positive Rate;
KNN	K-Nearest Neighbour.
LR	Logistic Regression;
ML	Machine Learning;
P	Precision;
ROC	Receiver Operating Characteristic;
ReLU	Rectified Linear Unit;
RF	Random Forest;
SVC	Support Vector classifier;
TNR	True Negative Rate;
TPR	True Positive Rate;
WHO	World Health Organization.

References

1. Epidemiology Working Group for NCIP Epidemic Response, Chinese Center for Disease Control and Prevention.

The epidemiological characteristics of an outbreak of 2019 novel coronavirus diseases (COVID-19) in China (Chinese). *Zhonghua Liu Xing Bing Xue Za Zhi* 2020; 41(2): 145–151. doi: 10.3760/cma.j.issn.0254-6450.2020.02.003
2. Rustam F, Reshi AA, Mehmood A, et al. COVID-19 future forecasting using supervised machine learning models. *IEEE Access* 2020; 8: 101489–101499. doi: 10.1109/ACCESS.2020.2997311
3. Malhotra P, Gupta S, Koundal D, et al. Deep learning-based computer-aided pneumothorax detection using chest X-ray images. *Sensors* 2020; 22(6): 2278. doi: 10.3390/s22062278
4. Cennimo DJ. Coronavirus disease 2019 (COVID-19) clinical presentation. Available online: https://emedicine.medscape.com/article/2500114-clinical#b2 (accessed on 1 August 2023).
5. X-ray (Radiography)-Chest, 2020. Available online: https://www.radiologyinfo.org/en/info/chestrad (accessed on 1 November 2022).
6. Sharma S, Gupta S, Gupta D, et al. Performance evaluation of the deep learning based convolutional neural network approach for the recognition of chest X-ray images. *Frontiers in Oncology* 2020; 12: 932496. doi: 10.3389/fonc.2022.932496
7. Ahmad M. Ground truth labeling and samples selection for hyperspectral image classification. *Optik* 2021; 230: 166267. doi: 10.1016/j.ijleo.2021.166267
8. Kayalibay B, Jensen G, van der Smagt P. CNN-based segmentation of medical imaging data. *arXiv* 2017; arXiv:1701.03056. doi: 10.48550/arXiv.1701.03056
9. Li Q, Cai W, Wang X, et al. Medical image classification with convolutional neural network. In: Proceedings of 2014 13th International Conference on Control Automation Robotics & Vision (ICARCV); 10–12 December 2014; Singapore. pp. 844–848.
10. Umer M, Sadiq S, Ahmad M, et al. A novel stacked CNN for malarial parasite detection in the blood smear images. *IEEE Access* 2020; 8: 93782–93792. doi: 10.1109/ACCESS.2020.2994810
11. Rouhi R, Jafari M, Kasaei S, et al. Benign and malignant breast tumors classification based on region growing and CNN segmentation. *Expert Systems with Applications* 2015; 42(3): 990–1002. doi: 10.1016/j.eswa.2014.09.020
12. Sharif M, Khan MA, Rashid M, et al. Deep CNN and geometric features-based gastrointestinal tract diseases detection and classification from wireless capsule endoscopy images. *Journal of Experimental & Theoretical Artificial Intelligence* 2019; 33(4): 577–599. doi: 10.1080/0952813X.2019.1572657
13. Asada N, Doi K, MacMahon H, et al. Potential usefulness of an artificial neural network for differential diagnosis of interstitial lung diseases: Pilot study. *Radiology* 1990; 177(3): 857–860. doi: 10.1148/radiology.177.3.2244001
14. Katsuragawa S, Doi K. Computer-aided diagnosis in chest radiography. *Computerized Medical Imaging and Graphics* 2007; 31(4–5): 212–223. doi: 10.1016/j.compmedimag.2007.02.003
15. Esteva A, Kuprel B, Novoa RA, et al. Dermatologist-level classification of skin cancer with deep neural networks. *Nature* 2017; 542: 115–118. doi: 10.1038/nature21056
16. Dong D, Tang Z, Wang S, et al. The role of imaging in the detection and management of COVID-19: A review. *IEEE Reviews in Biomedical Engineering* 2020; 14: 16–29. doi: 10.1109/RBME.2020.2990959
17. Wang L, Wong A. COVID-Net: A tailored deep convolutional neural network design for detection of COVID-19 cases from chest X-ray images. *arXiv* 2020; arXiv:2003.09871. doi: 10.48550/arXiv.2003.09871
18. Apostolopoulos ID, Mpesiana TA. COVID-19: Automatic detection from X-ray images utilizing transfer learning with convolutional neural networks. *Physical and Engineering Sciences in Medicine* 2020; 43: 635–640. doi: 10.1007/s13246-020-00865-4
19. Abbas A, Abdelsamea MM, Gaber MM. Classification of COVID-19 in chest X-ray images using DeTraC deep convolutional neural network. *arXiv* 2020; arXiv:2003.13815. doi: 10.48550/arXiv.2003.13815
20. Narin A, Kaya C, Pamuk Z. Automatic detection of coronavirus disease (COVID-19) using X-ray images and deep convolutional neural networks. *Pattern Analysis and Applications* 2021; 24(3): 1207–1220. doi: 10.1007/s10044-021-00984-y
21. Islam MZ, Islam MM, Asraf A. A combined deep CNN-LSTM network for the detection of novel coronavirus (COVID-19) using X-ray images. *Informatics in Medicine Unlocked* 2020; 20: 100412. doi: 10.1016/j.imu.2020.100412
22. Shorfuzzaman M, Masud M, Alhumyani H, et al. Artificial neural network-based deep learning model for COVID-19 patient detection using X-ray chest images. *Journal of Healthcare Engineering* 2021; 2021: 5513679. doi: 10.1155/2021/5513679
23. Mooney P. Chest X-ray images (Pneumonia). Available online: https://www.kaggle.com/datasets/paultimothymooney/chest-xray-pneumonia (accessed on 1 August 2023).
24. Shorten C, Khoshgoftaar TM. A survey on image data augmentation for deep learning. *Journal of Big Data* 2019; 6: 60. doi: 10.1186/s40537-019-0197-0
25. Ho D, Liang E, Liaw R. 1000x Faster data augmentation. Available online: https://bair.berkeley.edu/blog/2019/06/07/data_aug/ (accessed on 1 August 2023).
26. Mane DT, Kulkarni UV. A survey on supervised convolutional neural network and its major applications. *International Journal of Rough Sets and Data Analysis* 2017; 4(3): 71–82. doi: 10.4018/IJRSDA.2017070105
27. Liaw A, Wiener M. Classification and regression by randomForest. *R News* 2002; 2: 18–22.

28. Rustam F, Reshi AA, Ashraf I, et al. Sensor-based human activity recognition using deep stacked multilayered perceptron model. *IEEE Access* 2020; 8: 218898–218910. doi: 10.1109/ACCESS.2020.3041822
29. Kaur N, Jindal N, Singh K. A passive approach for the detection of splicing forgery in digital images. *Multimed Tools Application* 2020; 79(43): 32037–32063. doi: 10.1007/s11042-020-09275-w
30. Kaur N, Jindal N, Singh K. A deep learning framework for copy-move forgery detection in digital images. *Multimedia Tools and Applications* 2023; 82: 17741–17768. doi: 10.1007/s11042-022-14016-2
31. Kaur N, Jindal N, Singh K. An improved approach for single and multiple copy-move forgery detection and localization in digital images. *Multimedia Tools and Applications* 2022; 81(27): 38817–38847. doi: 10.1007/s11042-022-13105-6
32. Lau KW, Wu QH. Online training of support vector classifier. *Pattern Recognition* 2003; 36(8): 1913–1920. doi: 10.1016/S0031-3203(03)00038-4
33. Dreiseitl S, Ohno-Machado L. Logistic regression and artificial neural network classification models: A methodology review. *Journal of Biomedical Informatics* 2002; 35(5–6): 352–359. doi: 10.1016/S1532-0464(03)00034-0